# Grid-based quantum Monte-Carlo method for fermion systems

Alexander A. Kunitsa

Department of Chemistry, University of Illinois at Champaign-Urbana,

600 South Matthews Ave, Urbana, Illinois, 61801, USA

We present an extension of the diffusion Monte-Carlo algorithm allowing to simulate the quantum states of the few-fermion systems beyond the fixed node approximation. We addressed the negative sign problem by confining sign-carrying random walkers to the points of a uniform infinite spatial grid, allowing them to meet and annihilate in order to establish the nodal structure of the target state. The walker dynamics is governed by the imaginary time propagator, derived from an approximate discretized Hamiltonian and can be described as a non-gaussian branching random walk. The accuracy of the resulting stochastic representation of a fermion wave function is only limited by resolution of a grid and imaginary time-step, and can be improved in a controlled manner. We illustrate the method performance for a series of model problems including fermions in harmonic traps as well as the He atom in the triplet ground state. For the latter case the energy estimates were obtained with sub-millihartree statistical error without invoking the importance sampling transformation, yet were subject to the bias due to non-zero grid spacing.

## I. INTRODUCTION

Stochastic algorithms hold a potential to improve the performance of correlated real space electronic structure models by addressing the problem of dimensionality inherent in such calculations. Real space second-order Møller-Plesset perturbation theory [1] (MP2) and approximate coupled cluster methods with single and double excitations [2] (CC2) describe electron correlation in terms of two-particle pair functions satisfying inhomogeneous partial differential equations of Sinanoglu type [1]. Numerical approaches commonly used to obtain solutions of the equations, rely on the grid expansions [2–6] of the target six-dimensional quantities and suffer from the memory overheads. This problem can be tackled by Monte-Carlo sampling of the pair functions, however most of the existing stochastic algorithms [7–9]

(except for lattice regularized Diffusion Monte-Carlo, LRDMC [10, 14]) cannot be directly applied in a grid-based setting and make use of the fixed-node approximation [8, 11, 12] to avoid the negative sign problem [13].

The objective of this work is to introduce an extension of the Diffusion Monte-Carlo (DMC) method [8] capable of sampling discretized wave functions expanded on infinite Cartesian grids beyond the fixed-node approximation.

Similar to LRDMC, our algorithm relies on a finite difference approximation for the kinetic energy operator to represent the molecular Hamiltonian on the infinite uniform grid, yet does not impose nodal constraints [8, 11, 12] to ensure the convergence of the Monte-Carlo iterations to the target state with correct nodal structure. The latter is achieved by propagating sign carrying random walkers and performing their cancellation by analogy with Full Configuration Interaction Quantum Monte-Carlo (FCIQMC) [15, 16]. This feature distinguishes our method from previously developed fermion Monte-Carlo approaches that enforce cancellation by walker pairing, correlated dynamics and other techniques [17–23]. In contrast, grid-based simulation setup renders the collision probabilities of the walkers with opposite signs non-zero and gives rise to an unbiased cancellation scheme. The typical population dynamics pattern observed in our simulations is identical to that of FCIQMC and reflects the interplay between the first order spawning and second order cancellation processes [24]. Similar to FCIQMC, our algorithm produces the correct nodal structure of the target state provided the total number of walkers exceeds a critical value $N_c$ depending on a grid spacing, the dimension of configuration space and the character of the target state. Therefore, the value of $N_c$ determines the memory requirements for the grid-based Monte-Carlo simulations. In this work, we investigate the factors affecting the magnitude of $N_c$ for a series of model fermion systems in order to assess feasibility of the algorithm for the real space electronic structure calculations.

The manuscript is structured as follows. We present a closed form expression of the grid propagator and a detailed description of our Monte-Carlo method in Sec. II. The results of benchmark calculations on fermions in harmonic traps as well as singlet and triplet ground states of the helium atom are reported in Sec. III A and Sec. III B, respectively. We conclude the paper with the brief overview of the algorithmic aspects of the method and outline the directions of the future work.

## II. THEORY AND ALGORITHMS

We consider a Hamiltonian with a local spin-independent potential $V(r_1, r_2, ..., r_N)$:

$$H = -\frac{1}{2}\sum_{i=1}^{N}\Delta_i + V(r_1, r_2, ..., r_N) \tag{1}$$

We discretize the Laplacian on a uniform grid with spacing $\delta$ using central three point finite difference formula:

$$\Delta_i = \Delta_i^\delta + O(\delta^2), \tag{2}$$

where $\Delta_i^\delta$ is a symmetric lattice operator defined by the following expression ($x_i, y_i, z_i$ is a set of spatial coordinates and $s_i$ is a spin label):

$$\begin{aligned}\Delta_i^\delta f(x_i, y_i, z_i, s_i) =& \frac{f(x_i+\delta, y_i, z_i, s_i) + f(x_i-\delta, y_i, z_i, s_i) - 2f(x_i, y_i, z_i, s_i)}{\delta^2} + \\ & x_i \leftrightarrow y_i \leftrightarrow z_i\end{aligned} \tag{3}$$

Replacing $\Delta_i$ with their lattice approximations $\Delta_i^\delta$ one can introduce a grid Hamiltonian $H_\delta$. The action of the associated imaginary time propagator $e^{-\tau(H_\delta-\omega)}$ ($\omega$ and $\tau$ are energy onset and imaginary timestep, respectively) on a discretized wave function $\Psi$ can be evaluated using Suzuki-Trotter formula [25] in the limit $\tau \to 0$:

$$\begin{aligned}\Psi_\tau(r_1, s_1; ...; r_N, s_N) =& e^{-\tau\frac{V_0-\omega}{2}} \sum_{d_1,...,d_N} \Omega_{d_1,...,d_N} \Psi(r_1 - d_1\delta, s_1; ...; r_N - d_N\delta, s_N) \\ & + O(\tau^2),\end{aligned} \tag{4}$$

where $V_0 = V(r_1, ...r_N)$ and $\Omega_{d_1,...,d_N}$ is an amplitude, defined as a product of a spawning factor $m_{d_1,...,d_N} = e^{-\tau\frac{V(...,x_i+d_i^x\delta,y_i+d_i^y\delta,z_i+d_i^z\delta,...)-\omega}{2}}$ and a transition probability $P_{d_1,...,d_N} = \prod_{i=1}^{N} p_{d_i^x} p_{d_i^y} p_{d_i^z}$:

$$\Omega_{d_1,...,d_N} = e^{-\tau\frac{V(...,x_i+d_i^x\delta,y_i+d_i^y\delta,z_i+d_i^z\delta,...)-\omega}{2}} \prod_{i=1}^{N} p_{d_i^x} p_{d_i^y} p_{d_i^z} \tag{5}$$

The sum in Eq. 4 runs over all possible combinations of N three-dimensional lattice vectors $d_i$ with integer coordinates. Factors $p_d$ appearing in Eq. 5 can be calculated using the following formula:

$$p_d = \frac{1}{2\pi}\int_{-\pi}^{\pi} \cos(kd) e^{-\frac{2\tau}{\delta^2}\sin^2(k/2)} dk \tag{6}$$

$p_d$ describes a transition probability of a non-gaussian random walk on a one-dimensional lattice. This interpretation is supported by the properties of $p_d$:

1. For $\tau = 0$ $p_d = \delta_{d0}$

2. $p_d \geq 0$

3. $\sum_{d=-\infty}^{\infty} p_d = \frac{1}{2\pi} \int_{-\pi}^{\pi} \sum_{d=-\infty}^{\infty} e^{ikd} e^{-\frac{2\tau}{\delta^2} \sin^2(k/2)} dk = \int_{-\pi}^{\pi} \delta(k) e^{-\frac{2\tau}{\delta^2} \sin^2(k/2)} dk = 1$

In the limit $\delta \to 0$, $p_d$ converges to the transition probability of a gaussian random process in continuous space:

$$p_d \to \frac{1}{2\pi} \int_{-\infty}^{\infty} e^{ikd - \frac{1}{2\delta^2}\tau k^2} dk = \frac{\delta}{\sqrt{2\pi\tau}} e^{-\frac{d^2\delta^2}{2\tau}} \tag{7}$$

Eq. 7 follows from Eq. 6 by applying a saddle point approximation [26] to the integral in the vicinity of $k = 0$. Therefore, in the limit $\delta \to 0$ the lattice propagator reduces to the DMC evolution operator, which is consistent with $H_\delta \xrightarrow[\delta \to 0]{} H$.

The sum in Eq. 4 contains the terms that differ only by the interchange of particles with identical spin labels and are therefore equivalent up to the phase. This can be systematically accounted for by introducing a standard ordering of the grid nodes and permuting particle coordinates such that the list of occupied nodes conforms to the chosen order within the groups of particles with the same spin label.

The expression of the grid propagator gives rise to a simple algorithm capable of sampling antisymmetric wave functions expanded on a uniform grid by propagating a collection of random walkers in discretized space. Each walker is associated with a list of particle coordinates and is carrying a unit weight $c = \pm 1$. The particles are assigned fixed spin labels $s_i$ such that the spin projection $S_z$ of the target state is $S_z = \sum_{i=1}^{N} s_i$. A random walker changes sign, whenever the exchange of the two particles with the same spin label occurs in the course of propagation.The calculation work-flow is similar to that of DMC [8, 9] and includes the following steps:

1. **Initialization**. Initial walker positions are sampled from an N-particle discretized trial wave function $|\Psi_T(r_1, ..., r_N)|$. Sampling is performed using a standard Metropolis algorithm with a proposal distribution chosen to avoid Coulomb singularities if applicable. The signs of walkers coincide with the signs of $\Psi_T$.

2. **Generation of a transition probability list** Transition probabilities $p_d$ are computed using numerical quadrature from Eq. 6 and stored in a list along with the associated integer displacements $d$. This calculation is performed only once at the beginning of a Monte-Carlo run.

3. **Propagation and spawning** Each walker performs a branching random walk with hopping probabilities $P_{d_1,...,d_N} = \prod_{i=1}^{N} p_{d_i^x} p_{d_i^y} p_{d_i^z}$. The propagation step is executed by looping over the list of walkers $W$ and displacing walker coordinates by 3N dimensional vectors $(d_1\delta, ..., d_N\delta)$ sampled from $P_{d_1,...,d_N}$. If the new set of occupied grid points is unordered, the order is restored by applying a permutation $P$. The walker weight is multiplied by $(-1)^{[P]}$, where $[P]$ is the parity of $P$. Examples of sign-flipping and sign-preserving moves are presented in Fig. 1 for a simple case of two fermions in two-dimensional space.

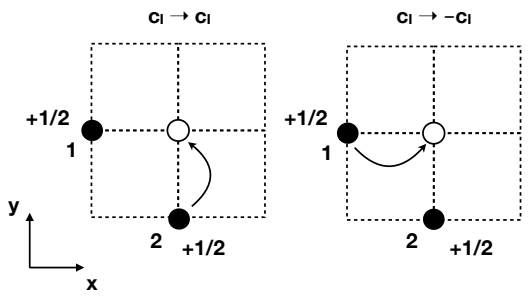


FIG. 1: Examples of sign-flipping (right panel) and sign-preserving (left panel) Monte-Carlo moves for two fermions with spin labels $s_i = +1/2$ (i = 1,2) in two-dimensional space. The grid nodes are assumed to follow dictionary order such that $(x, y) > (x', y')$ either if $x > x'$ or if $x = x'$ and $y > y'$

After the coordinate update is completed for a given walker, the old $\vec{r}^{old} = (r_1^{old}, r_2^{old}, ..., r_N^{old})$ and the new set of the particle coordinates $\vec{r}^{new} = (r_1^{old} + d_1\delta, r_2^{old} + d_2\delta, ..., r_N^{old} + d_N\delta)$ are used to calculate the branching factor $m = e^{-\tau \frac{V(\vec{r}^{old}) + V(\vec{r}^{new}) - 2\omega}{2}}$. The walker is then replaced by $\lfloor m + \xi \rfloor$ copies, where $\xi$ is a random number sampled for a uniform distribution on the interval $[0, 1]$.

4. **Annihilation** The new list $W'$ is sorted and searched for walkers occupying the same grid nodes. The weights of a group of walkers sharing the same grid point are combined to give a total weight $g$. The group is replaced by $|g|$ walkers with the weights equal to $sign(g)$.

5. **Measure the energy** The energy offset $\omega$ is updated to keep the number of walkers approximately constant $\omega \to \omega + 1/\tau \ln[N(W)/N(W')]$, where $N(W)$ and $N(W')$ are the sizes of the old and new walker lists, respectively. The mean value of $\omega$ in the

limit $\tau \to \infty$ can be used to estimate the ground state energy (growth estimator [27], $E_{gr} = \langle \omega \rangle$). Statistical accuracy considerations suggest that it is desirable to have another measure of the total energy (projected estimator [15, 28], $E_{proj}$) defined as follows:

$$E_{proj}(\tau) = \frac{\sum_i H_\delta \Psi_T(r_1^i, ...r_N^i)c_i}{\sum_i \Psi_T(r_1^i, ...r_N^i)c_i}, \tag{8}$$

where $r_k^i$ represents a position of k-th particle associated with i-th walker, $c_i$ is a corresponding weight and $\Psi_T$ is a trial function non-orthogonal to the target state.

The computational cost of the Monte-Carlo iteration is dominated by walker annihilation step which exhibits N log N scaling with the number of walkers due to the need to sort the walker list and presents an obstacle to a scalable parallel implementation of the algorithm. The memory requirements are proportional to the critical number of walkers $N_c$ and depend on walker annihilation rate. In the next section, it will be shown that the lack of cancellation leads to node sampling errors and gives rise to a bias in the calculated energy [15].

## III. RESULTS AND DISCUSSION

The performance of the method was studied for a series of model fermion systems chosen to demonstrate its applicability to the cases of both smooth and singular (Coulomb) potentials as well as to quantify the dependence of the critical number of walkers on the grid spacing. The primary focus of our studies was on the two-particle systems in three-dimensional space in view of potential applications of the algorithm in the context of real space MP2 and CC2 calculations. All simulations were performed using a three-point central finite difference approximation for the kinetic energy operator. Transition probabilities were calculated numerically using Clenshaw-Curtis adaptive quadrature algorithms implemented in GNU scientific library [29]. Displacements with the probabilities $\leq 10^{-8}$ were discarded. The spatial grid was chosen to have the same spacing along X, Y and Z directions. Statistical errors of the energy estimators were evaluated using blocking analysis [30] as implemented in pyblock module [31].

### A. Fermions in Harmonic traps

We considered a system of four independent spin-1/2 particles confined in a one dimensional harmonic trap represented by a potential of the form $V = 1/2 \sum_{i=1}^{4} x_i^2$, where $x_i$ are particle

coordinates. Stochastic algorithm presented in Sec. II was used to sample the lowest energy states of the system with the total spin $S$ equal to 0, 1, and 2. The simulation was performed on a grid with spacing $\delta = 0.1$ a.u. The initial particle coordinates were sampled from a uniform distribution within a 6.0 a.u. cubic box. In order to mitigate the population control bias [27] we propagated a large ensemble of $10^7$ random walkers with the imaginary time step 0.1 a.u. for the total of 5000 Monte-Carlo steps. Upon convergence, the target state energy was measured by the growth estimator. The main sources of error in the calculated energies were therefore due to the finite time step and non-zero grid spacing, the latter precluding direct comparison with the known exact results in continuous space. For benchmarking purposes, reference energy values were evaluated as the sums of one particle energies obtained by diagonalizing discretized harmonic oscillator Hamiltonian on a uniform grid spanning the interval $[-L, L]$, where $L = 6.0$ a.u. and were converged up to at least eight decimal places. As shown in Table I, the differences between Monte-Carlo energy estimates and the reference values are within 3 mH which can be attributed to the time step error (SI, to be added).

TABLE I: Energies of the spin states of the system of four spin-1/2 fermions in 1-D harmonic trap (grid spacing 0.1 a.u.). See the main text for the details of DMC simulations

| Spin | $E_{gr}$, a.u. | $E_{exact}$, a.u. |
|---|---|---|
| 0 | 3.99458 ± 0.00004 | 3.996246 |
| 1 | 4.99168 ± 0.00004 | 4.993740 |
| 2 | 7.98292 ± 0.00005 | 7.986223 |

In order to study the dependence of the energy estimates on the cancellation rate we performed a series of simulations for walker ensembles of varying sizes. The simulation results presented in Fig. 2 (Panel A) indicate that calculated energies converge to reference values provided the frequency of cancellation events or, equivalently, the total number of walkers exceeds a threshold value $N_c$ depending on the character of the target state. The lack of cancellation manifests itself in the values of the growth estimator below the true ground state energy. The rate of convergence tends to decrease for high spin states which can be attributed to the relatively diffuse character of their wave function due to occupation of high energy one particle states. The population dynamics curves presented in Fig. 2 (Panel B) are reminiscent

of those obtained in FCIQMC [15] and similarly exhibit pronounced plateaus corresponding to $N_c$ values. This feature reflects the competition between the spawning and walker cancellation process [24].

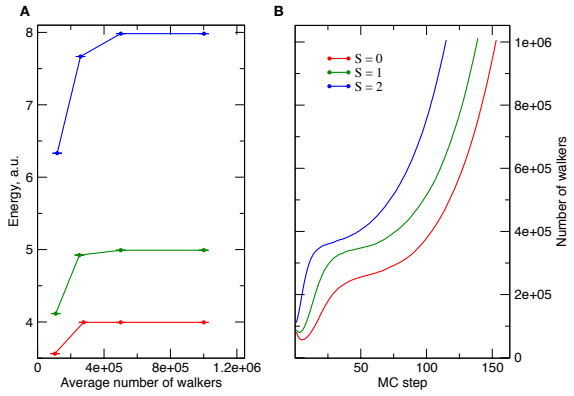


FIG. 2: The dependence of the growth estimator on the average number of walkers for the lowest spin states of 4 fermions in a one-dimensional harmonic trap (A). The typical population dynamics pattern in a grid-based quantum Monte-Carlo run. The energy onset was set to 4.25, 5.25, and 8.25 for the states with spin 0, 1, and 2, respectively and kept fixed during the propagation. (B)

The effects of grid spacing on the critical number of walkers were analyzed for a triplet system of two spin-1/2 fermions in a 3-D harmonic trap. Due to the larger dimension of the configuration space the critical number of walkers is an order of magnitude higher compared to the previously considered system and exhibits a steep growth with $\delta$ (Fig. 3). The least square fit of the $\ln N_c$ - $\ln \delta$ dependence suggests that $N_c \approx 339\delta^{-5.994}$. In general, one could expect $N_c \propto \delta^{-Nd}$, where N is the number of particles and d is the dimension of one-particle configuration space.

### B. $^3S$ state of Helium atom

Monte-Carlo simulation of Coulomb systems requires modifications of the algorithm to account for the singularities of the potential energy operator. In contrast to continuous DMC, random walks in discretized space have a non-zero probability of visiting coincidence planes (i.e. the regions of space where $r_i = r_j$ for some pair of electrons) as well as electron-nucleus coalescence points, leading to the diverging branching factors. In order to avoid divergences,

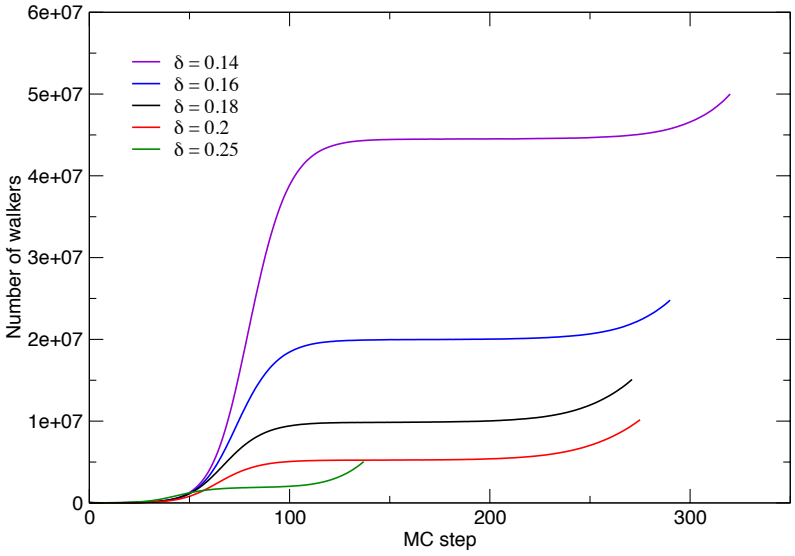


FIG. 3: Population dynamics for two spin-1/2 fermions in a 3-D harmonic trap for several grid spacings $\delta$. The calculations were performed for the energy onset $\omega = 4.5$ a.u. and imaginary time-step $\delta t = 0.1$ a.u.

we placed the nucleus of He atom at the point with coordinates $(\delta/2, \delta/2, \delta/2)$, where $\delta$ is the grid spacing, and terminated the random walks leading to coinciding electron coordinates. The reference energy values were obtained from the fixed-node grid-based Monte-Carlo simulations using exact nodal surface of the $^3S$ state [32]. The nodal constraints were imposed by killing the random walkers attempting to acquire a sign inconsistent with that of a trial wave function with exact node, i.e. the walker weight $c_i$ was set to 0 whenever $c_i \times \vec{\Psi}_T(r_1^i, r_2^i) < 0$, where $\Psi_T$ had the following form:

$$\Psi_T(r_1, r_2) = e^{\left(\frac{r_{12}}{2(1+br_{12})}\right)} A(1,2)\{(2 - Zr_2)e^{-Z\times(r_1+0.5r_2)}\},$$

where $r_i$ (i = 1,2) denote electron-nucleus distance and $A(1,2) = \frac{1}{2}(1 - P_{12})$ is anti-symmetrization operator, parameters b and Z were set to 0.2 and 1.95, respectively. Simulations were performed for the ensemble of 10000 walkers and imaginary time step dt = 0.005 a.u. The energy was measured by the projection estimator to reduce statistical errors. The results of the grid-based fixed node calculations for the $^3S$ state of He atom are presented in Fig. 4 (Left

panel).

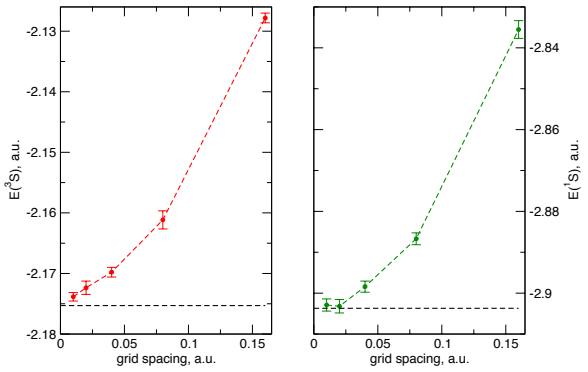


FIG. 4: Energies of the $^3S$ (Left panel) and $^1S$ (Right panel) states of He atom as a functions of grid spacing. Statistical errors are shown with vertical bars. Horizontal dashed lines indicate the exact energy of the states estimated from experimental data (-2.1753 a.u. and -2.9036 for $^3S$ and $^1S$, respectively)

Fixed-node energy of the $^3S$ state of He exhibits slow convergence with the grid spacing, being in error of 1.5 mH to the exact value for $\delta = 0.01$ a.u. Comparison with the results obtained for a nodeless $^1S$ state (Fig. 4, Right panel) suggests that this can be attributed to inherent inefficiency of a uniform grid in representing electron-electron and electron-nuclear cusps [5]. Interestingly, the grid acts to suppress the fluctuations of the branching factor by preventing the walkers from closely approaching the nucleus and gives rise to the order of magnitude smaller statistical errors compared to similar continuous space calculations [23]. Note, that the bias due to the finite grid spacing decreased monotonously with $\delta$ in the range from 0.16 to 0.01 a.u. For finer grids the character of convergence is hard to discern as it is masked by statistical errors.

Grid-based Monte-Carlo simulations beyond fixed-node approximation were performed for two grid spacings, $\delta = 0.16$ and $\delta = 0.08$. In both cases the convergence with respect to the number of walkers was ensured by performing the calculation for walker ensembles of varying sizes and checking the stability of the energy estimates. Additionally, the average fraction of walkers $w$ with correct signs (i.e. with the sign consistent with $\Psi_T$) was recorded during Monte-Carlo runs. The calculation results are presented in Table. II along with the fixed-node

energies for the same grid spacings.

TABLE II: Energies of the $^3S$ state of He atom obtained from grid-based DMC calculations without nodal constraints. Fixed-node results are presented for reference purposes.

| $\delta$ | $< N >$ | $w$ | E, a.u. | fixed node |
|---|---|---|---|---|
| 0.16 | 35027070 | 0.979 | -2.12695 $\pm$ $10^{-5}$ | N |
| 0.16 | 70489775 | 0.983 | -2.12687 $\pm$ $10^{-5}$ | N |
| 0.16 | 10000 | 1.00 | -2.1278 $\pm$ 0.001 | Y |
| 0.08 | 615787933 | 0.967 | -2.16126 $\pm$ $10^{-5}$ | N |
| 0.08 | 625057844 | 0.968 | -2.16169 $\pm$ $10^{-5}$ | N |
| 0.08 | 10008 | 1.00 | -2.1612 $\pm$ 0.0015 | Y |

The values of $w$ close to 1.0 indicate the convergence of the Monte-Carlo iteration to the state with nearly exact nodal structure. Energy estimates obtained from the simulations without nodal constraints are in excellent agreement with the reference fixed-node data within the statistical error bars. The critical number of walkers in our simulations exceeded 6 $10^8$ for the case of the fine grid ($\delta$ = 0.08 a.u.) indicating that in its present form the algorithm is impractical beyond two-particle systems in three dimensional space. However, moderate memory requirements and monotonous decrease of the grid-induced bias in the calculated energies with the grid spacing makes it a promising alternative to the iterative schemes currently used for the real space MP2 and CC2 calculations.

## IV. SUMMARY AND CONCLUSIONS

We developed a novel grid-based algorithm enabling DMC simulations of the target states with arbitrary nodal structure without invoking the fixed-node approximation. To this end, the original continuous space problem was mapped onto its lattice fermion counterpart by representing the Hamiltonian on the infinite uniform spatial grid using a central finite difference approximation for the kinetic energy operator. The expression of the associated grid propagator is similar to that of continuous space DMC and reduces to it in the limit of zero grid spacing, yet describes a non-gaussian statistics of walker moves. The key component of the formalism is

the definition of random walkers which incorporates the permutational symmetry of the target state and can be extended to account for the point group symmetries. For a series of model systems we demonstrated that our Monte-Carlo algorithm converges to target states with the correct nodal structure, provided the total number of walkers exceeds a critical value $N_c$. As follows from the simulation results for the triplet state of He atom, realistic grid based Monte-Carlo calculations on two electron systems in three-dimensional space require the ensembles of $10^7 - 10^9$ walkers to achieve moderate accuracy of the energy estimates. For the latter simulation, the set of walker coordinates occupied 17 Gb of memory. Further reduction of the memory requirements can be achieved by utilizing spatial symmetry and extending the algorithm for the case of adaptive grids, which is currently under active exploration.

[1] O. Sinanolu, J. Chem. Phys. **36**, 3198 (1962).

[2] J. S. Kottmann and F. A. Bischoff, J. Chem. Theory Comput. **13**, 5945 (2017), URL https://doi.org/10.1021/acs.jctc.7b00694.

[3] T. Yanai, G. I. Fann, Z. Gan, R. J. Harrison, and G. Beylkin, J. Chem. Phys. **121**, 6680 (2004), URL https://aip.scitation.org/doi/abs/10.1063/1.1790931.

[4] R. J. Harrison, G. I. Fann, T. Yanai, Z. Gan, and G. Beylkin, J. Chem. Phys. **121**, 11587 (2004).

[5] F. A. Bischoff and E. F. Valeev, J. Chem. Phys. **139**, 114106 (2013).

[6] S. Hirata, T. Shiozaki, C. M. Johnson, and J. D. Talman, Mol. Phys. **115**, 510 (2017).

[7] M. H. Kalos, Phys. Rev. **128**, 1791 (1962), URL http://link.aps.org/doi/10.1103/PhysRev.128.1791.

[8] J. B. Anderson, J. Chem. Phys. **63**, 1499 (1975), ISSN 0021-9606, 1089-7690, URL http://scitation.aip.org/content/aip/journal/jcp/63/4/10.1063/1.431514.

[9] A. Lchow, WIREs Comput Mol Sci **1**, 388 (2011), ISSN 1759-0884, URL http://onlinelibrary.wiley.com/doi/10.1002/wcms.40/abstract.

[10] Michele Casula, Claudia Filippi, and Sandro Sorella, Phys. Rev. Lett. **95**, 100201 (2005).

[11] Peter J. Reynolds and David M. Ceperley, J. Chem. Phys. **77**, 5593 (1982), ISSN 0021-9606, URL http://aip.scitation.org/doi/abs/10.1063/1.443766.

[12] D. J. Klein and H. M. Pickett, J. Chem. Phys. **64**, 4811 (1976), ISSN 0021-9606, 1089-7690, URL http://scitation.aip.org/content/aip/journal/jcp/64/11/10.1063/1.432043.

[13] M. Troyer and U.-J. Wiese, Phys. Rev. Lett. **94**, 170201 (2005).

[14] M. Casula, S. Moroni, S. Sorella, and C. Filippi, J. Chem. Phys. **132**, 154113 (2010).

[15] George H. Booth, Alex J. W. Thom, and Ali Alavi, J. Chem. Phys. **131**, 054106 (2009), ISSN 0021-9606, URL http://aip.scitation.org/doi/full/10.1063/1.3193710.

[16] D. Cleland, G. H. Booth, and A. Alavi, J. Chem. Phys. **132**, 041103 (2010), ISSN 0021-9606, URL http://aip.scitation.org/doi/10.1063/1.3302277.

[17] J. Carlson and M. H. Kalos, Phys. Rev. C **32**, 1735 (1985), URL http://link.aps.org/doi/10.1103/PhysRevC.32.1735.

[18] M. H. Kalos and K. E. Schmidt, J. Stat. Phys. **89**, 425 (1997), ISSN 0022-4715, 1572-9613, URL http://link.springer.com/article/10.1007/BF02770774.

[19] M. H. Kalos, Phys. Rev. E **53**, 5420 (1996), URL http://link.aps.org/doi/10.1103/PhysRevE.53.5420.

[20] M. H. Kalos and F. Pederiva, Phys. Rev. Lett. **85**, 3547 (2000), URL https://link.aps.org/doi/10.1103/PhysRevLett.85.3547.

[21] James B. Anderson, Carol A. Traynor, and Bruce M. Boghosian, J. Chem. Phys. **95**, 7418 (1991), ISSN 0021-9606, 1089-7690, URL http://scitation.aip.org/content/aip/journal/jcp/95/10/10.1063/1.461368.

[22] Y. Mishchenko, Phys. Rev. E **73**, 026706 (2006), URL http://link.aps.org/doi/10.1103/PhysRevE.73.026706.

[23] D. Coker and R. O. Watts, Mol. Phys. **58**, 1113 (1986).

[24] Spenser J. S., J. Chem. Phys. **136**, 054110 (2012), ISSN 0021-9606, URL http://aip.scitation.org/doi/10.1063/1.3681396.

[25] H. F. Trotter, Proc. Amer. Math. Soc. **10**, 545 (1959), URL https://mathscinet.ams.org/mathscinet-getitem?mr=0108732.

[26] J. Mathews and R. L. Walker, *Mathematical Methods of Physics* (W.A. Benjamin, New York, 1970), 2nd ed., ISBN 978-0-8053-7002-7.

[27] C. J. Umrigar, M. P. Nightingale, and K. J. Runge, J. Chem. Phys. **99**, 2865 (1993), ISSN 0021-9606, URL http://aip.scitation.org/doi/abs/10.1063/1.465195.

[28] G. An and J. M. J. van Leeuwen, Phys. Rev. B **44**, 9410 (1991), URL http://link.aps.org/doi/10.1103/PhysRevB.44.9410.

[29] M. G. et al., *Gnu scientific library reference manual (3rd ed.)*, URL http://www.gnu.org/software/gsl/.

[30] H. Flyvbjerg and H. G. Petersen, J. Chem. Phys. **91**, 461 (1989).

[31] J. Spencer, *pyblock: python module for performing blocking analysis on data containing serial correlations*, original-date: 2014-04-02T02:12:30Z, URL https://github.com/jsspencer/pyblock.

[32] Dario Bressanini and Peter J. Reynolds, Phys. Rev. Lett. **95**, 110201 (2005).